THE ROYAL SOCIETY

Received 21 October 2002
Accepted 3 December 2002
Published online 28 February 2003

Plankton blooms induced by turbulent flows

R. Reigada[1*], R. M. Hillary[2], M. A. Bees[3], J. M. Sancho[4] and F. Sagués[1]

[1]*Departament de Quimica-Fisica, Universitat de Barcelona, Avinguda Diagonal 647, 08028 Barcelona, Spain*
[2]*Renewable Resources Assessment Group, Centre for Environmental Technology, Imperial College of Science, Technology and Medicine, London SW7 1NA, UK*
[3]*Department of Mathematics, University of Glasgow, 15 University Gardens, Glasgow G12 8QW, UK*
[4]*Departament d'Estructura i Constituents de la Materia, Universitat de Barcelona, Avinguda Diagonal 647, Barcelona 08028, Spain*

Plankton play an important role in the ecology of the ocean and the climate because of their participation in the global carbon cycle at the base of the food chain. However, damaging plankton blooms can sometimes occur and are initially characterized by sudden transient increases in the phytoplankton population. They are thought to be driven by several effects, such as seasonal variations in temperature and salinity, and nutrient mixing. Furthermore, phytoplankton and zooplankton have different buoyancy properties, leading to a differential response in turbulent environments. In this paper, we investigate this effect in a model of advected plankton dynamics. We find that, over a range of parameter values, flows of marine species subjected to inertial/viscous forces naturally lead to patchiness and, in turn, periodically sustained plankton blooms.

Keywords: plankton patchiness; plankton blooms; inertial and viscous effects

1. INTRODUCTION

Plankton patchiness has been observed on a wide range of spatial and temporal scales (Franks 1997; Abraham 1998; Folt & Burns 1999) and has been attributed to a range of physical and biological mechanisms. It is important to understand both the mechanisms that result in patchiness and the effect of patchiness on food-web interactions, which can have a major impact on fisheries policy (Legendre 1990).

All oceanic organisms experience advection by turbulence but what effect this has on the population dynamics and the distribution of organisms is unclear. Turbulence typically consists of an amalgam of coherent and other structures, which can cause inhomogeneous distributions of passively advected organisms, with novel spatial statistics when reaction dynamics are also considered (Abraham 1998). However, it has become clear that we cannot necessarily consider plankton simply to be passive as they have some motile abilities (Folt & Burns 1999) as well as differing viscous and inertial properties to the surrounding fluid (Squires & Yamazaki 1995). In other words, plankton can move and have different material properties to sea water. The spatial and temporal scales can, to some degree, dictate which of these characteristics, if any, are quantitatively significant. However, it is conceivable that small qualitative effects may have a great impact on the subsequent planktonic dynamics.

Recent results suggest that differing aggregation zones exist for particles advected by complex flows if their densities and material properties vary slightly from the surrounding fluid (Squires & Eaton 1991; Reigada *et al.* 2001). In particular, light particles are generally forced into areas of large vorticity while heavier particles tend to be constrained to regions with high strain rates. The full dynamics of inertial particles in a general flow are highly non-trivial (Maxey & Riley 1983) and a variety of additional effects occur. For plankton, if one variety of organism is lighter than the other we may have some degree of separation of predator and prey.

At moderate spatial scales phytoplankton 'blooms' can occur, whereby the population of phytoplankton rapidly increases in number and remains at this level for some period of time before returning to normal. This is the hallmark of an excitable system. Truscott & Brindley (1994) investigated a two-component phytoplankton–zooplankton (PZ) model that has the characteristics of an excitable system whose excitability is robust over a realistic parameter range. Normally, however, a large driving perturbation is required to initiate the bloom in general for an excitable system. Possibly, many mechanisms such as variations in salinity, temperature and nutrient mixing are responsible for this initiation. Furthermore, the breaking of excitation waves by shear flow has been proposed (Biktashev *et al.* 1998) as a possible mechanism for plankton patchiness. Similarly, a chaotically advected excitable system, together with a driving influx of nutrient (in this case iron), has been investigated as an alternative mechanism (Neufeld *et al.* 2002). In both cases, the system needs some non-vanishing perturbation to seed the excitation.

We explore the effects of inertia on advected excitable PZ dynamics. In particular, we shall address the question of whether the differential flow of phytoplankton and zooplankton is sufficient to seed a bloom. This scenario would require no extraneous perturbation to drive the excitation. In other words, after sufficient inertial separation a large population of the phytoplankton might be allowed to grow in certain localized regions with minimal predation and this, coupled with dispersive effects, may constitute the supra-threshold perturbation necessary for an excitable

*Author for correspondence (reigada@qf.ub.es).

system. Also, we investigate what consequences this may have on the distribution of the organisms and the predator–prey contact rates.

Of especial interest in this paper are length-scales of kilometres and time-scales of days. In particular, we do not directly investigate or incorporate individual-based plankton–plankton interactions (except via measurements of relative flux) and biased motile responses owing to food availability, predation or reproduction (Folt & Burns 1999), although the slow drift and micropatchiness associated with these mechanisms may also have qualitative effects over very large times.

We shall employ a statistical approach to generate turbulent flows using techniques previously applied to a variety of physical systems (Marti *et al.* 1997). The advantages are that one has complete control over the statistical properties of the flow.

2. TURBULENT ADVECTION OF INERTIAL ORGANISMS

The assumption that zooplankton and phytoplankton can be treated as passive scalars is, at best, hopeful. They can both, to varying degrees, have different viscous and inertial properties to the surrounding fluid. In Maxey & Riley (1983) the equation of motion was derived for a spherical particle at position $\mathbf{X}_n$ with velocity $\mathbf{V}_n$, where n is the particle index, in a non-stationary fluid velocity field, $\mathbf{U}(\mathbf{X}_n)$:

$$m_{\mathrm{p}}\frac{\mathrm{d}\mathbf{V}_n}{\mathrm{d}t} = m_{\mathrm{f}}\frac{D\mathbf{U}(\mathbf{X}_n)}{Dt} + 6\pi a\mu(\mathbf{U}(\mathbf{X}_n) - \mathbf{V}_n) - \frac{m_{\mathrm{f}}}{2}\left(\frac{\mathrm{d}\mathbf{V}_n}{\mathrm{d}t} - \frac{\mathrm{d}\mathbf{U}(\mathbf{X}_n)}{\mathrm{d}t}\right) - 6\pi a^2\mu\int_{-\infty}^{t}\frac{\mathrm{d}(\mathbf{V}_n - \mathbf{U}(\mathbf{X}_n))/\mathrm{d}\tau}{(\pi\nu(t-\tau))^{1/2}}\mathrm{d}\tau, \tag{2.1}$$

where m_{p} is the particle mass and m_{f} is the mass of the volume of fluid displaced by the particle; ν and μ are the kinematic and dynamic viscosities, respectively, associated with the surrounding fluid and a is the radius of the particle. The first term in equation (2.1) is the Bernoulli term, which is the force from the undisturbed flow, the second term is the Stokes viscous drag, the third is the added mass term and the final term is the Basset history force. This equation incorporates the assumption that the particle, associated Reynolds number and fluid gradients around the particle surface are small (Maxey & Riley 1983). Invoking some other common approximations that can be found in the literature (Druzhinin & Ostrovsky 1994; Taylor 1923; Auton *et al.* 1988; Reigada *et al.* 2001) one obtains the following reduced version of equation (2.1):

$$\frac{\mathrm{d}\mathbf{V}_n}{\mathrm{d}t} = A(\mathbf{U}(\mathbf{X}_n) - \mathbf{V}_n) + R\frac{D\mathbf{U}(\mathbf{X}_n)}{Dt}. \tag{2.2}$$

In this equation we have non-dimensionalized the time by rescaling it using the flow time-scale, $t \rightarrow tu_0/l_0$ (we keep the same notation for simplicity). Here, $A = \alpha l_0/u_0$ is the dimensionless version of the inertia parameter $\alpha = (12\pi a\mu)/(2m_{\mathrm{p}} + m_{\mathrm{f}})$, which corresponds to the balance between viscous and inertial forces. The Bernouilli parameter $R = 3m_{\mathrm{f}}/(2m_{\mathrm{p}} + m_{\mathrm{f}})$ introduces the ratio between masses.

Later, we shall move to a Eulerian frame so we need to establish the existence of a corresponding Eulerian velocity field. To obtain a simplified, long-time expression for the corrected velocity field of the dispersed species we follow the approach first employed in Maxey (1987) for the singular case of heavy particles, and later generalized by Reigada *et al.* (2001). It amounts to the assumption that A is large so that after the formal integration of equation (2.2) we can ignore any exponential transients, and retain only terms up to the first order in A^{-1}. If we assume that the ambient flow is stationary, $\mathbf{U}(\mathbf{r}, t) = \mathbf{U}(\mathbf{r})$, we obtain the effective velocity field, $\mathbf{V}(\mathbf{r})$ as

$$\mathbf{V}(\mathbf{r}) = \mathbf{U}(\mathbf{r}) + \frac{R-1}{A}[\mathbf{U}(\mathbf{r})\cdot\nabla]\mathbf{U}(\mathbf{r}) + \mathcal{O}(A^{-2}). \tag{2.3}$$

The important result already contained in equation (2.3) is that particles drift from the flow trajectories and tend to aggregate in various zones depending on their material characteristics. The aggregation of particles occurs in regions of negative divergence, $\nabla\cdot\mathbf{V} < 0$, for a set particle class (in contrast to neutrally buoyant, passively advected particles). The divergence of equation (2.3) can be written in terms of the squares of the magnitudes of the local strain rate and the local vorticity, S^2 and $|\Omega|^2$, respectively, of the original turbulent flow, $\mathbf{U}$. Hence,

$$\nabla\cdot\mathbf{V} = \frac{R-1}{A}\left(2S^2 - \frac{|\Omega|^2}{2}\right), \tag{2.4}$$

which leads to two different possibilities for aggregation. If the organism is heavy ($R < 1$), then accumulation occurs in regions where $S^2 > |\Omega|^2/4$, regions of high strain and low vorticity (outside the eddies). Conversely, if an organism is lighter than the surrounding medium ($R > 1$) accumulation occurs in regions where $S^2 < |\Omega|^2/4$, areas with high vorticity and low strain (inside the eddies).

Let us now introduce our model for turbulent flows. We refer to a statistically homogeneous, isotropic and stationary two-dimensional velocity field $\mathbf{U}$ as first introduced in Marti *et al.* (1997). This fluid flow is generated with regard to three basic well-defined statistical properties: u_0^2 is the intensity of the flow, l_0 is the length correlation of the flow and t_0 is the time correlation of the flow. These kinematic characteristics are expressed in terms of the velocity correlation function, which in turn depends on the form of the energy spectrum. For the flow used in this paper we shall adopt Kraichnan's spectrum (Kraichnan 1970) as it describes a turbulent flow velocity field that incorporates a wide band of excited modes, but whose energy drops off sharply for large wavenumbers. This is ideal for this application as it allows us to additionally model planktonic dispersion at smaller scales (see later). Moreover, Kraichnan's spectrum exhibits a well-defined peak at a wavenumber of $k = k_0$. Other spectra such as that due to Kárman–Obukhov (von Kárman 1948) with a long '$-5/3$' tail can be similarly applied, but one must be careful to properly (and not overly) account for planktonic dispersion processes at small spatial scales.

Maxey & Riley (1983) indicate guidelines for the proper application of equation (2.1). The main condition is that $(a^2u_0)/(l_0\nu) \ll 1$. Because, typically, $a < 10^{-2}$ m, $u_0 = 0.1$

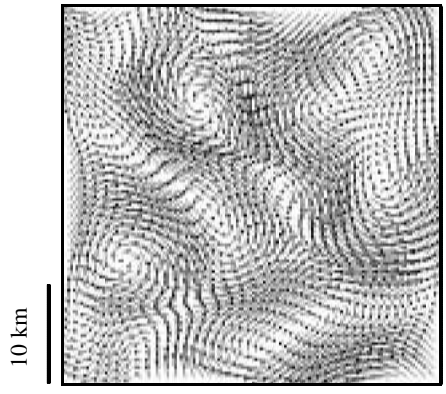

Figure 1. Snapshot of the 'frozen' turbulent velocity field employed in the simulations.

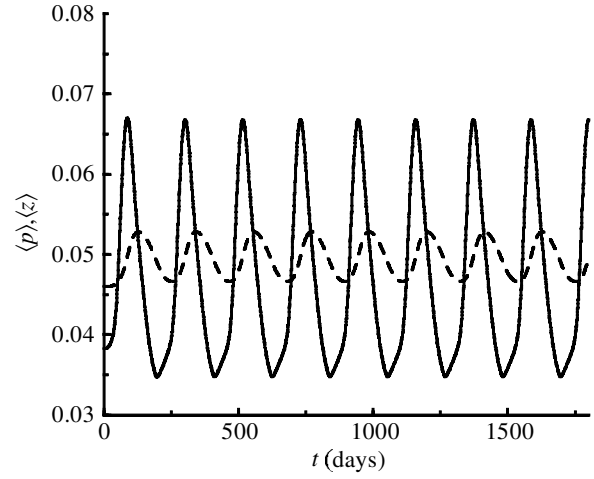

Figure 2. Oscillatory bloom in the mean concentrations of phytoplankton and zooplankton. Solid line, $\langle p\rangle$; dashed line, $\langle z\rangle$.

m s^{-1}, $l_0 = 5 \times 10^4$ m and $\nu = 10^{-6}$ m^2 s^{-1} we can safely apply the Maxey & Riley equation (see later for a full discussion of parameter values). In line with a realistic range of values for α (Squires & Yamazaki 1995) we assume, henceforth, that $\alpha = 0.0257$ s^{-1}, which means that the zooplankton radius is *ca*. 1 cm and implies that $A \gg 1$, justifying the preceding analysis.

Although the general method of flow generation allows us to work with a non-stationary field, we shall not make use of the possibility in this paper. For the sake of simplicity, and to avoid the existence of many temporal scales, we take a frozen flow, with u_0 and l_0 as the only flow parameters. In figure 1 we show the flow realization used in our simulations.

3. A MODEL FOR ADVECTED EXCITABLE PLANKTON DYNAMICS

Following Truscott & Brindley (1994) we use the following rate laws for the PZ interactions that, in essence, model logistic phytoplankton growth, Holling type III grazing by zooplankton and a linear higher-predatory response with regard to the zooplankton mortality:

$$\mathscr{T}_P(P,Z) = rP\left(1 - \frac{P}{K}\right) - \frac{\gamma Z P^2}{P^2 + \kappa^2},$$
$$\mathscr{T}_Z(P,Z) = \frac{\mathrm{e}\gamma Z P^2}{P^2 + \kappa^2} - \delta Z. \qquad (3.1)$$

We further couple the above rate laws to an advection–diffusion scheme to represent the effects of planktonic interactions and diffusion/motility in a Eulerian frame-of-reference. We non-dimensionalize the resulting equations such that $P = Kp$, $Z = Kz$, $x = l_0\tilde{x}$, $y = l_0\tilde{y}$, $t = \tau l_0/u_0$, $\mathbf{V}^i = u_0\mathbf{v}^i$, $d_i = D_i/(u_0 l_0)$, with $\mathbf{V}^i$ obtained from equation (2.2) with appropriate choices of $R = R_\mathrm{p}$ and R_z, and D_i representing turbulent diffusivities (assumed equal, see below). After eliminating the tildes this gives us the following non-dimensional scheme:

$$\frac{\partial p}{\partial \tau} = -\nabla\cdot(\mathbf{v}^p p - d_\mathrm{p}\nabla p) + \beta p(1-p) - \frac{\bar{\gamma} z p^2}{p^2 + \chi^2},$$
$$\frac{\partial z}{\partial \tau} = -\nabla\cdot(\mathbf{v}^z z - d_z\nabla z) + \varepsilon\left(\frac{\bar{\gamma} z p^2}{p^2 + \chi^2} - \sigma z\right), \qquad (3.2)$$

where the dimensionless parameters of the excitable model are defined as $\beta = rl_0/u_0$, $\varepsilon = \mathrm{e}$, $\chi = \kappa/K$, $\sigma = \delta l_0/(\varepsilon u_0)$ and $\bar{\gamma} = \gamma l_0/u_0$.

We choose L, the simulation box size, to be 50 km (where l_0 is related to L in the sense that l_0 determines the scale of the eddies, and in this case we choose $L \approx 10l_0$; see figure 1) and the characteristic velocity to be $u_0 = 0.1$ m s^{-1}, similar to that used in both Abraham (1998) and Neufeld *et al.* (2002). From Truscott & Brindley (1994), we take $\beta = 0.162$, $\chi = 0.053$, $\sigma = 0.130$ and $\varepsilon = 0.05$ (hence, the zooplankton population is the slow/recovery variable). Our choice of l_0 and u_0 are such that we can realistically fix $\bar{\gamma} = 1$ and, hence, the reaction effects are comparable to advective effects.

Kraichnan's spectrum has a maximum occurring at $k = 0.75$ and decreases to a very small value at $k = 2$. Hence, the length-scale associated with the highest energy is equal to $2\pi/0.75 = 8.4$, or about one-tenth of the length of the simulation region. The length-scale associated with a wavenumber of 2 (residual energy) is given by $2\pi/2 = \pi$, or about one-twentieth of the simulation region. If the simulation region is 50 km then the dimensional length-scale associated with low spectral energy is $L/20 = 2.5 \times 10^5$ cm. This is the length-scale for which we wish to implement a turbulent diffusivity in the reaction–advection–diffusion system. Hence, the diffusivity $D = 0.01 * l^{1.15} = 1.6 \times 10^4$ cm^2 $s^{-1} = 1.6$ m^2 s^{-1} (according to the empirical relationship extracted by Okubo (1971) from experimental data). Therefore, the synthetic turbulence accounts for the large-scale flow centred about a wavenumber k_0. The energy spectrum drops off sufficiently quickly for larger wavenumbers such that the turbulent mixing can be modelled by simple diffusion at small length-scales (several grid points).

We neglect any swimming diffusion for the following reason. If we assume an upper bound on the typical swimming speed, $V_s = \mathscr{O}(10^{-1})$ m s^{-1}, and some typical reorientation time-scale, $\tau_r = \mathscr{O}(1)$ s, then the diffusion can be approximated by $D_s \approx V_s^2\tau_r$, which is $\mathscr{O}(10^{-2})$ m^2 s^{-1} (also, see data for algal cells; Hill & Hader (1997)), and is significantly smaller than the turbulent diffusivity calculated above.

The system is spatially discretized using a square lattice of 128 × 128 cells, with a grid spacing of 0.5, and the time-step used in the numerical scheme is $\Delta t = 0.0002$. The

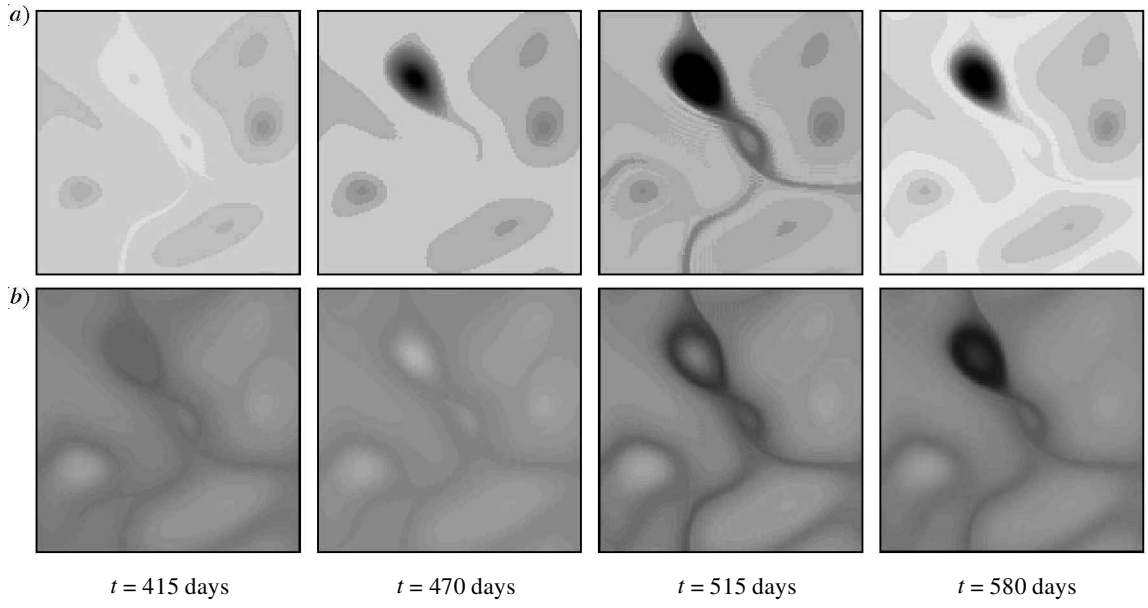

Figure 3. Snapshots of the (*a*) phytoplankton and (*b*) zooplankton distribution during the oscillatory bloom. For snapshots of phytoplankton, white refers to $p = 0$, and for p greater than or equal to 0.6 black is used. For zooplankton, white refers to $z = 0$ and black implies that z is greater than or equal to 0.1.

integration of equation (3.2) was achieved by using a two-step Lax–Wendroff scheme (Press *et al.* 1992) that gave good numerical convergence for the parameter values employed.

We begin from a homogeneous initial distribution of both species in their unexcited, equilibrium concentration values $p^* = 0.038\ 27$ and $z^* = 0.046\ 03$. The inertial separation under turbulent advection is enough to perturb the equilibrium distribution and, analogous to the threshold nature of perturbations in excitable systems, we find that there exist critical values of the Bernoulli parameters which separate regimes where no bloom occurs from regions where localized excitation and subsequent bloom propagation results.

The most interesting cases occur for the regime where we have neutrally buoyant phytoplankton ($R_p = 1$) and slightly heavy zooplankton ($R_z = 0.9$). Here, indeed, we see the emergence of an oscillatory bloom in the average phytoplankton population with a period of *ca.* 210 days. Figure 2 presents the nature of the oscillatory bloom in the mean population values of phytoplankton and zooplankton, whereas in figure 3 one may observe the spatial evolution of the distribution of the phytoplankton population during one bloom cycle. The initial excitation is because of the inertial drift of zooplankton that moves out from the eddies initiating a phytoplankton bloom inside the vortices. The details of the behaviour of the planktonic populations and distributions are described in the following section. What is fascinating is that this regime is the most physically realistic scenario, as phytoplankton are usually close to neutrally buoyant, and zooplankton are slightly more dense than the surrounding ocean (McCave 1984; Squires & Yamazaki 1995; Folt & Burns 1999).

4. AGGREGATION, SEGREGATION AND CONTACT RATES

In this section, we explore the implications of bloom formation on the statistical properties of the organisms' spatial distributions, in relation to the recruitment of zooplankton. We employ some statistical measures, which are described below.

To measure the magnitude of aggregation of phytoplankton we define Π_p to be

$$\Pi_p = \frac{\langle p \rangle^2}{\langle p^2 \rangle}, \tag{4.1}$$

where $\langle \cdot \rangle$ denotes a spatial average, and similarly for Π_z for the zooplankton. If the distribution is homogeneous then $\Pi_p = 1$, whereas if all the phytoplankton are all at one point then $\Pi_p = 1/N^2$ (where N^2 is the number of mesh points in the computational grid).

Another statistic we wish to use is a measure of the predator–prey contact rate. It is derived from the difference in the relative fluxes of the phytoplankton and zooplankton, which provides a measure of the rate at which the two organisms 'meet'. In two dimensions, we find that the relative flux of phytoplankton past a zooplankter, at a given spatial location is given by

$$\Gamma_p(t) = 2\mathscr{R}\left\| \frac{\mathbf{J}_z}{z} - \frac{\mathbf{J}_p}{p} \right\| p, \tag{4.2}$$

where $\mathscr{R}$ is the zooplankton's perceptive radius. This is a local measure which might be used to assess the phytoplanktonic consumption by zooplankton at a particular point within a complex flow, and to compare zooplankton grazing strategies in turbulent environments (see the experiments of Marrasé *et al.* (1990)). Furthermore, the analogous expression for the normalized averaged contact rate, $\Gamma(t)$, is

$$\Gamma = 2\mathscr{R}\frac{\int_S \left\| p\mathbf{J}_z - z\mathbf{J}_p \right\| \mathrm{d}A}{\int_S z\mathrm{d}A \int_S p\mathrm{d}A}, \tag{4.3}$$

where S is the spatial domain under consideration. We

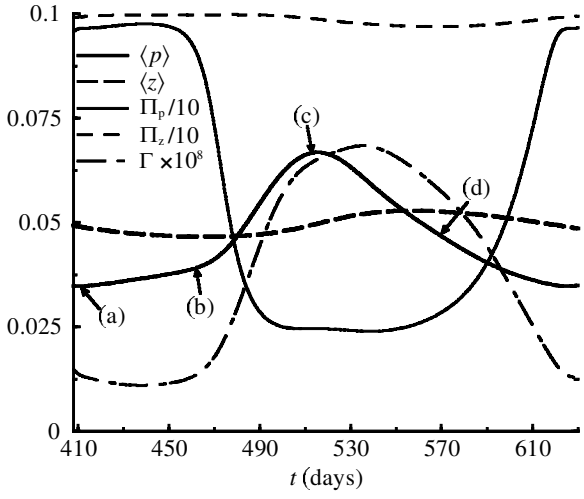

Figure 4. Complete view of one period of the oscillatory bloom (Case IV). The distribution of both species at times (a)–(d) in this plot are shown from left to right in figure 3.

use the value $\mathscr{R} = 6$ cm, in line with the suggestion of 2–4 body lengths from Folt & Burns (1999).

In figure 4 we observe how these statistical measures vary over the period of one bloom oscillation. From (a) to (b) in figure 4, the phytoplankton population slowly increases but mostly spreads (diffusion) inside the vortices unoccupied by zooplankton. During this period, Π_p stays close to 1 because there is not localization of phytoplankton but diffusion of these organisms inside the vortices. Besides, zooplankton decreases in the entire system owing to the lack of prey. This effect is especially enhanced inside the eddies because of their outward drift. The phytoplankton bloom begins at point (b). From (b) to (c) the lack of zooplankton allows the concentration of phytoplankton to increase quite dramatically, although it is always confined to the vortices. Hence, Π_p decreases to a low value, a signature of localization. At the same time, the zooplankton starts to grow because of the presence of large quantities of phytoplankton. This is also reflected in the sudden growth of the contact rate Γ just before phytoplankton reaches its maximum at (c). From (c) to (d), the large phytoplankton population contributes to the regeneration of the zooplankton, especially in the straining regions of the flow around the eddies where the phytoplankton had accumulated previously. For this reason, Π_z begins to decrease, a sign of zooplankton localization. The zooplankton grows even as the phytoplankton decreases (owing to the fast/slow nature of the PZ dynamics). At this stage, it can be observed how the zooplankton population penetrates (by growth and diffusion) into the eddies owing to the large localized concentration of phytoplankton, counteracting the effects of inertial drift. After point (d), to complete the oscillation, the zooplankton population begins to decay owing to the lack of prey, and the phytoplankton population returns to the initial state at (a). During this stage, localization of both species decreases, indicating more disperse distributions, and the contact rate decreases owing to a reduction in the area of cohabitation.

5. CONCLUSIONS

We have demonstrated how differential flow effects of phytoplankton and zooplankton, coupled with excitable reaction dynamics, may contribute towards oceanic phytoplankton blooms and patchiness. We have focused our efforts by employing an elementary excitable model for the planktonic interactions, although this does not preclude the possibility of similar behaviour emerging for more complex or realistic ecosystems. Upon advection by turbulence, heavy and light particles accumulate in separate areas of the flow, as phytoplankton and zooplankton have different viscous and inertial properties to the surrounding oceanic medium. Simple reaction dynamics then ensure that non-trivial patchiness results. Of particular interest was the oscillatory excitation, which occurred in the most realistic inertial regime (neutrally buoyant phytoplankton and slightly heavy zooplankton). The period of this oscillation was of the order of one year and occurred for a range of parameter values. The result is particularly intriguing owing to the resulting annual period of the blooms, although we would emphasize that seasonal forcing is likely to play a great role. Such seasonal forcing would consist of variations in temperature, light, nutrients (owing to mixing) or fluctuations in other components of the food chain. The important message in this work is that with a minimal model and using experimentally determined values for the parameters, we obtain a natural period of just less than one year, which may be further synchronized by the external forcing. This self-initiating, periodic patch-forming mechanism differs from other related work on advection-enhanced blooms (Biktashev *et al.* 1998; Neufeld *et al.* 2002) as it requires no initial perturbation and is self-sustaining.

In § 4 we investigated how bloom formation may affect the statistical properties of the spatial distribution of the organisms and the contact rates (of particular relevance to fish stocks). In principle, one should be able to compare the statistics resulting from these or other similar simulations with experimentally determined data (Okubo 1971; Marrasé *et al.* 1990; Powell & Okubo 1994). To measure contact rates we developed a continuum formulation based on the relative flux of the two species. This revealed interesting behaviour and emphasized the role of relative (inertially driven) flux in accentuating contact rates and, thus, grazing rates. In particular, it is clear that the spatially averaged grazing rate varies significantly in response to physical and population dynamical cues.

For populations of plankton subject to excitable dynamics and turbulent advection with inertial effects, the mean contact rate does depend on the extent of the patchiness in contrast to other approaches, such as the probabilistically derived results of Pitchford & Brindley (2001). Furthermore, the separation of the two organisms can be either good for the recruitment of zooplankton or bad. Although not shown in this paper, for an extreme case (very light phytoplankton and very heavy zooplankton), we observed that the contact rate decreased with time, as we would expect because predator and prey reside in different areas. In this case the phytoplankton accumulate in the eddies and the zooplankton move to low vorticity regions, reaching a steady, heterogeneous distribution of plankton. However, for the oscillatory case presented here, and cor-

responding to the more realistic situation, the bloom can periodically propagate, which allows for zooplankton to move into phytoplankton populated areas thus increasing the contact rate.

Finally, it is a priority of future research to ascertain the robustness of the above results subject to variations in the model or more realistic modelling approaches. The key requirements for the above-described mechanism are underlying excitability and the inertial separation of species in a complex flow. Furthermore, the inertial separation may play other interesting roles in non-excitable systems.

The authors acknowledge the support of this research by the Ministerio de Educacion y Cultura through project nos BFM2000-0624 and BXX2000-0638, and by the Comissionat per Universitats i Recerca de la Generalitat de Catalunya under project no. 1999SGR00041. R.M.H. is funded by an EPSRC research studentship. R.M.H. and M.A.B. gratefully acknowledge financial support from the EU Access to Research Infrastructure action of the *Improving Human Potential Programme* during collaborative visits to Barcelona.

REFERENCES

Abraham, E. R. 1998 The generation of plankton patchiness by turbulent stirring. *Nature* **39**, 577–580.

Auton, T. R., Hunt, J. C. R. & Prud'homme, M. 1988 The force exerted on a body in inviscid unsteady nonuniform rotational flow. *J. Fluid Mech.* **197**, 241–258.

Biktashev, V. N., Holden, A. V., Tsyganov, M. A., Brindley, J. & Hill, N. A. 1998 Excitation wave breaking in excitable media with linear shear flow. *Phys. Rev. Lett.* **81**, 2815–2818.

Druzhinin, O. A. & Ostrovsky, L. A. 1994 The influence of Basset force on particle dynamics in two-dimensional flows. *Physica* D **76**, 34–43.

Folt, C. L. & Burns, C. W. 1999 Biological drivers of zooplankton patchiness. *Trends Ecol. Evol.* **14**, 300–305.

Franks, P. J. S. 1997 Spatial patterns in dense algal blooms. *Limnol. Oceanogr.* **42**, 1297–1305.

Hill, N. A. & Hader, D. P. 1997 A biased random walk model for the trajectories of swimming micro-organisms. *J. Theor. Biol.* **186**, 503–526.

Kraichnan, R. H. 1970 Diffusion by a random velocity field. *Phys. Fluids* **13**, 22–31.

Legendre, L. 1990 The significance of microalgal blooms for fisheries and for the export of particulate organic carbon in oceans. *J. Plank. Res.* **12**, 681–699.

McCave, I. N. 1984 Size-spectra and aggregation of suspended particles in the deep ocean. *Deep-Sea Res.* **22**, 491–502.

Marrasé, C., Costello, J. H., Granata, T. & Strickler, J. R. 1990 Grazing in a turbulent environment: energy dissipation, encounter rates and efficiency of feeding currents in *Centropages hamatus*. *Proc. Natl Acad. Sci. USA* **87**, 1653–1657.

Marti, A. C., Sancho, J. M., Sagues, F. & Careta, A. 1997 Langevin approach to generate synthetic turbulent flows. *Phys. Fluids* **9**, 1078–1084.

Maxey, M. R. 1987 The gravitational settling of aerosol particles in homogeneous turbulence and random flow fields. *J. Fluid Mech.* **174**, 441–465.

Maxey, M. R. & Riley, J. J. 1983 Equation of motion for a small rigid sphere in a nonuniform flow. *Phys. Fluids* **26**, 883–889.

Neufeld, Z., Haynes, P. H., Gargon, V. C. & Sudre, J. 2002 Ocean fertilization experiments may initiate a large scale phytoplankton bloom. *Geophys. Res. Lett.* **29**, 1029–1035.

Okubo, A. 1971 Oceanic diffusion diagrams. *Deep-Sea Res.* **18**, 789–802.

Pitchford, J. W. & Brindley, J. 2001 Prey patchiness, predator survival and fish recruitment. *Bull. Math. Biol.* **63**, 527–546.

Powell, T. M. & Okubo, A. 1994 Turbulence, diffusion and patchiness in the sea. *Phil. Trans. R. Soc. Lond.* B **343**, 11–18.

Press, W. H., Teukolsky, S. A., Vetterling, W. T. & Flannery, B. P. 1992 *Numerical recipes in C*. Cambridge University Press.

Reigada, R., Sagues, F. & Sancho, J. M. 2001 Inertial effects on reactive particles advected by turbulence. *Phys. Rev.* E **64**, 026307/1–026307/9.

Squires, K. D. & Eaton, J. K. 1991 Preferential concentration of particles by turbulence. *Phys. Fluids* **3**, 1169–1178.

Squires, K. D. & Yamazaki, H. 1995 Preferential concentration of marine particles in isotropic turbulence. *Deep-Sea Res.* **142**, 1989–2004.

Taylor, G. I. 1923 Experiments on the motion of solid bodies in rotating fluids. *Proc. R. Soc. Lond.* A **104**, 213–218.

Truscott, J. E. & Brindley, J. 1994 Ocean plankton populations as excitable media. *Bull. Math. Biol.* **56**, 981–998.

von Kármán, T. V. 1948 Progress in the statistical theory of turbulence. *Proc. Natl Acad. Sci. USA* **34**, 530–539.